

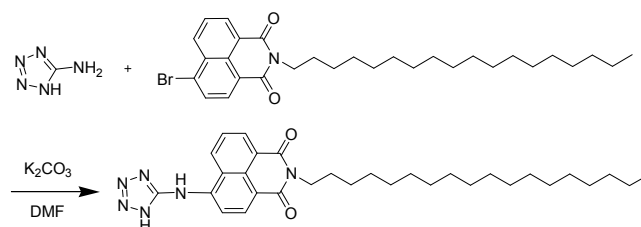
Multifunctional fluorescent naphthalimide self-assembly system for detection Cu^{2+} , K^+ and continuously sensing organic amines and gaseous acids

Xinhua Cao^{*a}, Yiran Li^a, Aiping Gao^a, Yongsheng Yu^a, Qiuju Zhou^a, Xueping Chang^{*a}, Xiaohan Hei^b

^aCollege of Chemistry and Chemical Engineering & Henan Province Key laboratory of Utilization of Non-metallic Mineral in the South of Henan, Xinyang Normal University, Xinyang 464000, China

^bCollege of municipal and environmental engineering, Henan University of Urban Construction, Pingdingshan 467000, China

*E-mail: caoxhchem@163.com



Scheme S1 The synthesis route of compound 1

Synthesis of compound 1: N-octadecyl-4-bromine-1, 8-naphthalimide (1.0 g, 1.89 mmol), 5-amino-1H-tetrazole (0.32 g, 3.78 mmol) and K_2CO_3 (0.52 g, 3.78 mmol) were mixed in DMF (30 mL). The reaction mixture was stirred for 12 h at 100 °C under N_2 atmosphere. After the reaction was over, DMF was removed under reduced pressure. The compound 1 as a brown powder was obtained through column chromatography (methanol/ CH_2Cl_2 , 1/100, v/v) with the yield of 25%; ^1H NMR (600 MHz, CDCl_3): δ 8.61 (d, $J = 7.8$ Hz, 1H), 8.54 (d, $J = 7.8$ Hz, 1H), 8.46 (d, $J = 7.8$ Hz, 1H), 7.72 (t, $J = 7.8$ Hz, 1H), 7.06 (t, $J = 7.8$ Hz, 1H), 4.16 (t, $J = 7.8$ Hz, 2H), 1.71 (m, 2H), 1.42-1.23 (m, 30H), 0.87 (t, $J = 7.2$, 3H); ^{13}C NMR (150 MHz, CDCl_3): δ 162.9, 131.0, 126.7, 41.7, 41.1, 37.8, 36.4, 29.5, 29.4, 29.2, 28.2, 27.1, 25.9. HRMS calculated for $\text{C}_{31}\text{H}_{45}\text{N}_6\text{O}_2$ $[\text{M}+\text{H}]^+$ 533.3604, found: 533.3661.

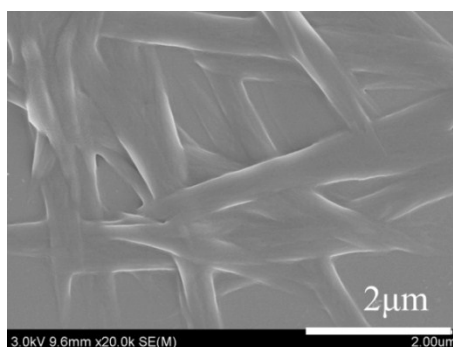


Fig. S1 SEM image of xerogel 1 from acetone/H₂O (1/1, v/v).

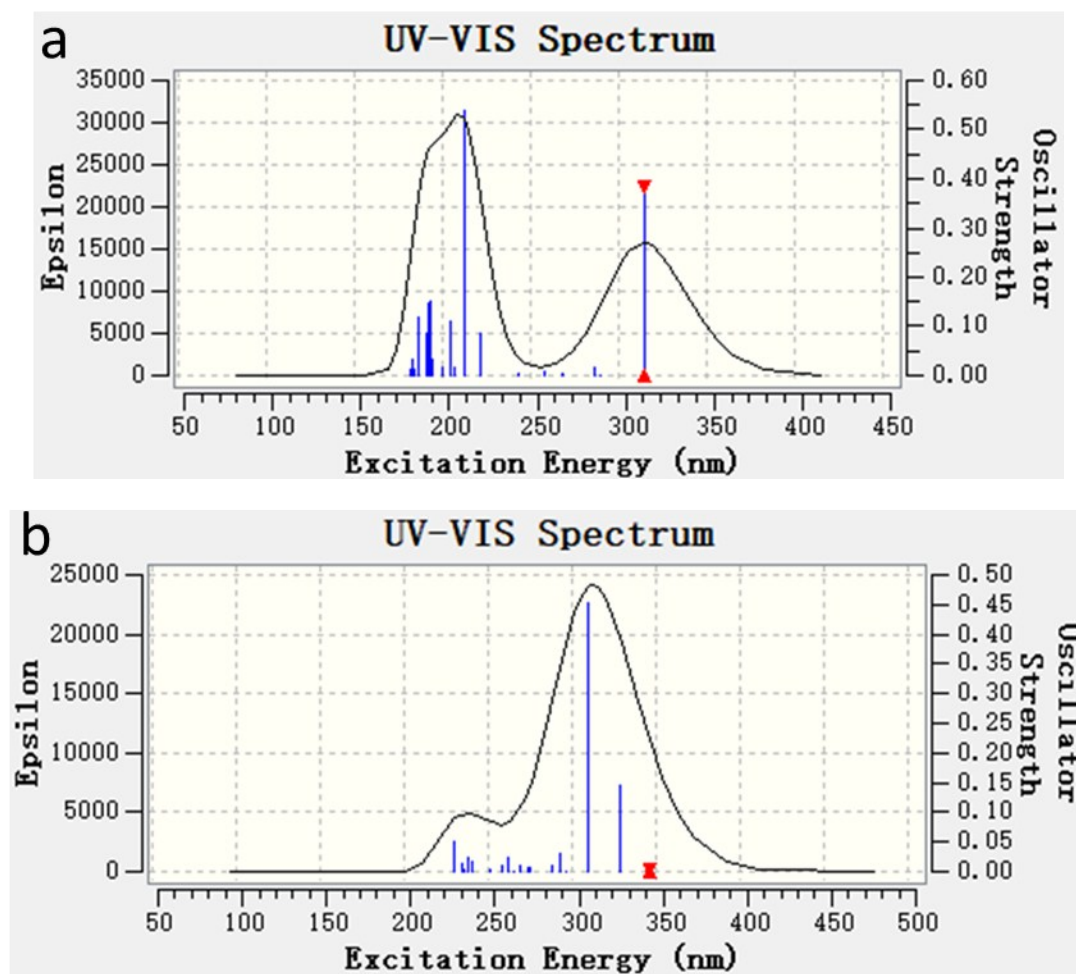
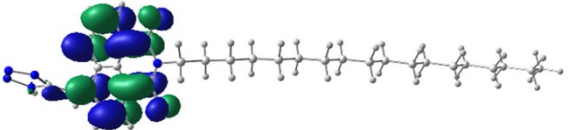
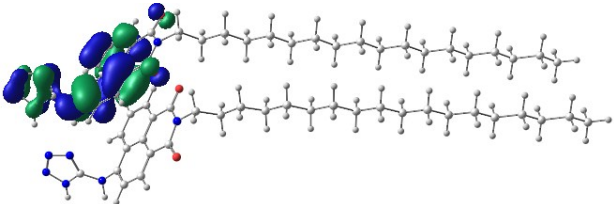
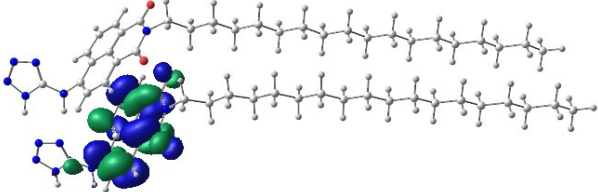


Fig. S2 The absorption spectra of compound 1 with single and dimer modes obtained from the DFT calculation: a) for single mode; b) for dimer mode.

Table S1 HOMOs and LUMOs distributions of the single and dimer of compound **1**.

Molecule	HOMOs and LUMOs distributions
single	 <p>HOMO -7.68 eV</p>
single	 <p>LUMO -1.37 eV</p>
dimer	 <p>HOMO -7.25 eV</p>
dimer	 <p>LUMO -1.79 eV</p>

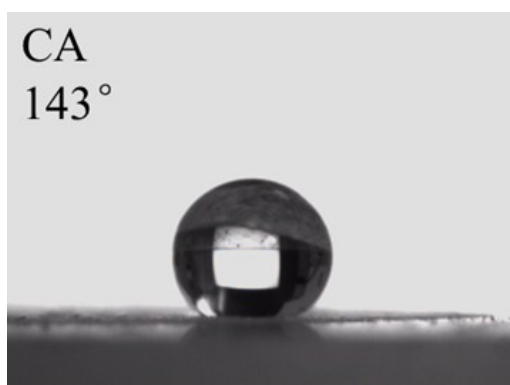


Fig. S3 Water contact angle experiment of xerogel **1** films formed in acetone/H₂O (1/1, v/v). The gel concentration was at their corresponding CGC.

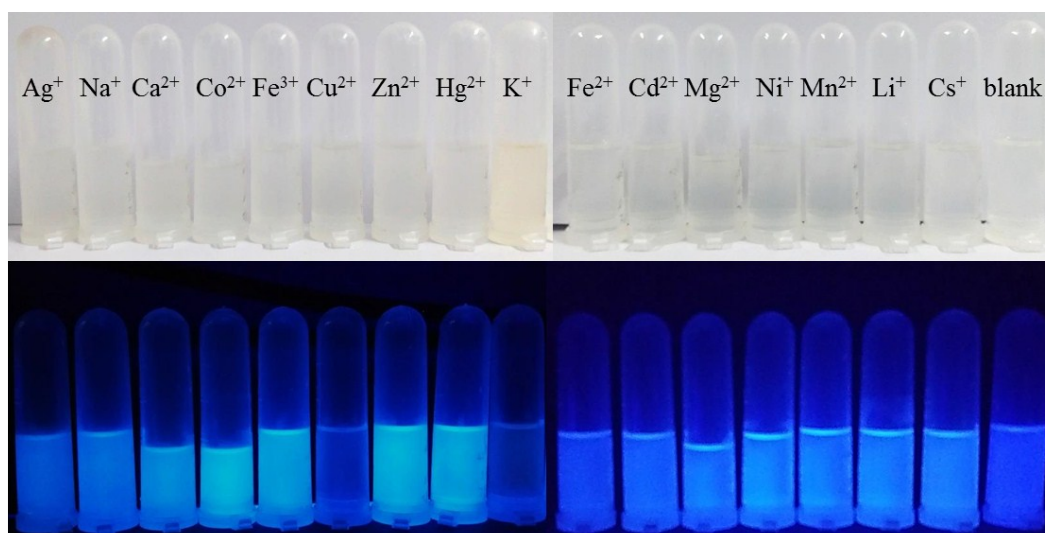


Fig. S4 Visual changes in color for compound **1** in acetone (10^{-5} M) with addition of different metal ions (1.0 eq.). The upper and lower were under daylight and 365 nm UV lamp, respectively.

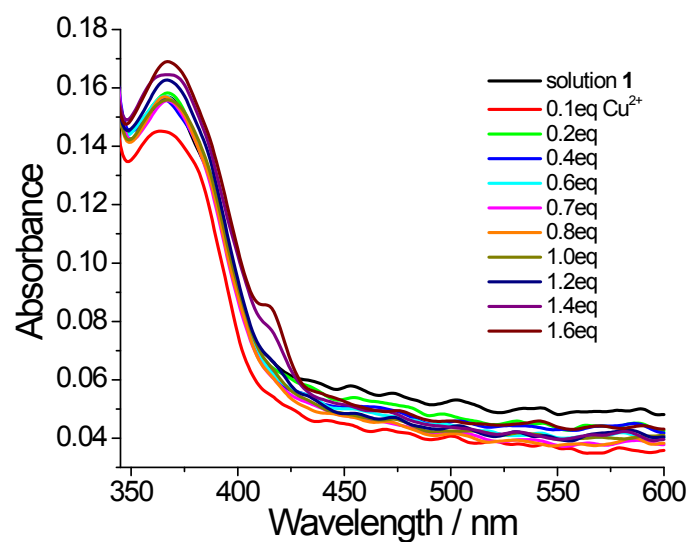


Fig. S5 UV-vis absorption spectra change of compound **1** in solution under the titration of Cu^{2+} . The concentration of solution **1** was at 10^{-5} M.

Table S2 Detection limit of **1** toward Cu^{2+} , K^+ , TEA and TFA in acetone by fluorescence emission changes at 436 nm

n (X _n)	1	2	3	4	5	6	7	8	9	10
intensity	5027.09	5027.43	5025.28	5026.37	5027.64	5027.28	5025.97	5025.20	5027.11	5027.10

$$X_{\text{average}} = 5026.65 \quad \sigma_{\text{wb}} = \sqrt{\frac{\sum (X_n - X_{\text{average}})^2}{n}} = 0.7053$$

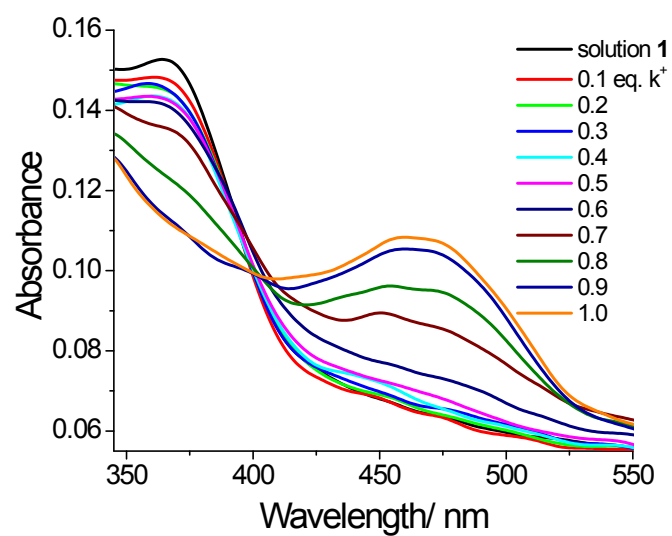


Fig. S6 UV-vis absorption spectra change of solution **1** in acetone (10^{-5} M) under the titration of K^+ .

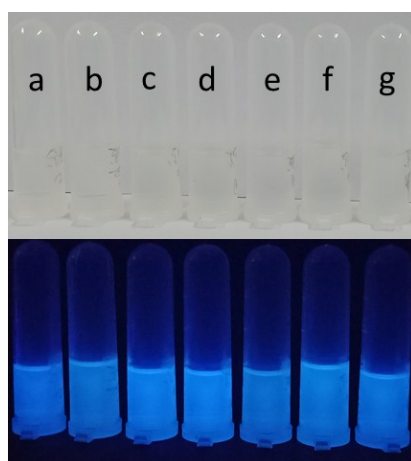


Fig. S7 Visual changes for solution **1** in acetone (10^{-5} M) with addition of different acids ($20\mu\text{L}$, 1M); (a) blank; (b) acetic acid; (c) HCl; (d) propionic acid (e) formic acid; (f) HNO_3 (g) TFA. The upper and lower were under daylight and 365 nm UV lamp, respectively.

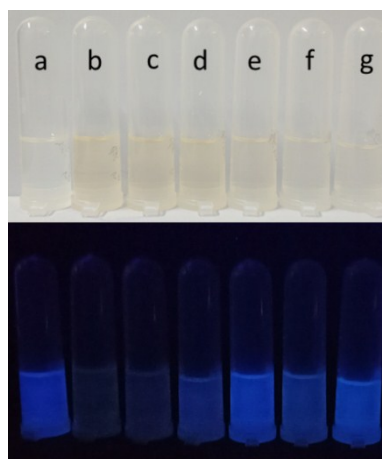


Fig. S8 Visual changes for solution **1** in acetone (10^{-5} M) with addition of different amines ($20\mu\text{L}$, 1M); (a) pyridine; (b) diethylamine; (c) ethanediamine; (d) TEA; (e) aniline (f) butylamine; (g) blank. The upper and lower were under daylight and 365 nm UV lamp, respectively.

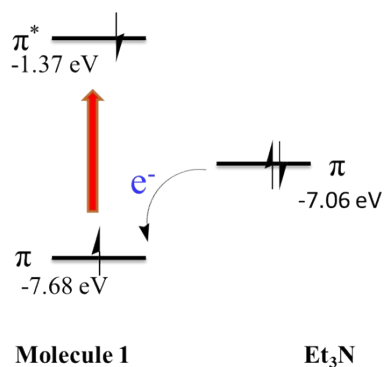


Figure S9 Energy levels of HOMO and LUMO orbital of compound **1** and Et₃N showing the favourable electron transfer from amine to the photo excited state of compound **1**. The same diagram applies to the other amines, while the reducing power (or the π -orbital level) would be different from that of Et₃N. Geometry optimization and energy calculation were performed with density-functional theory (B3LYP-D3/6-31G*) using G09 package.

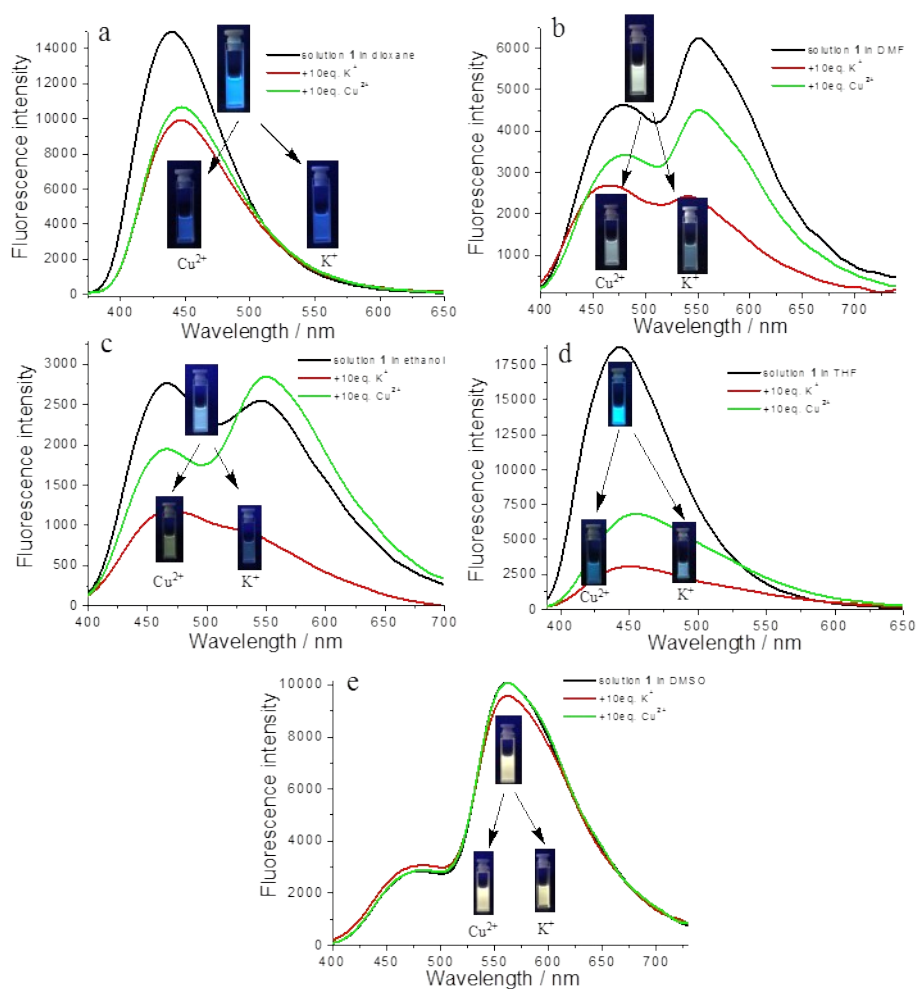


Fig. S10 Fluorescence emission change of solution **1** from different solvents under addition of Cu²⁺ and K⁺ at the excitation of 375 nm; a) for dioxane; b) for DMF; c) for ethanol; d) for THF and e) for DMSO. The concentration of solution **1** was 10⁻⁵ M. The addition amount of Cu and K was 10.0 eq.

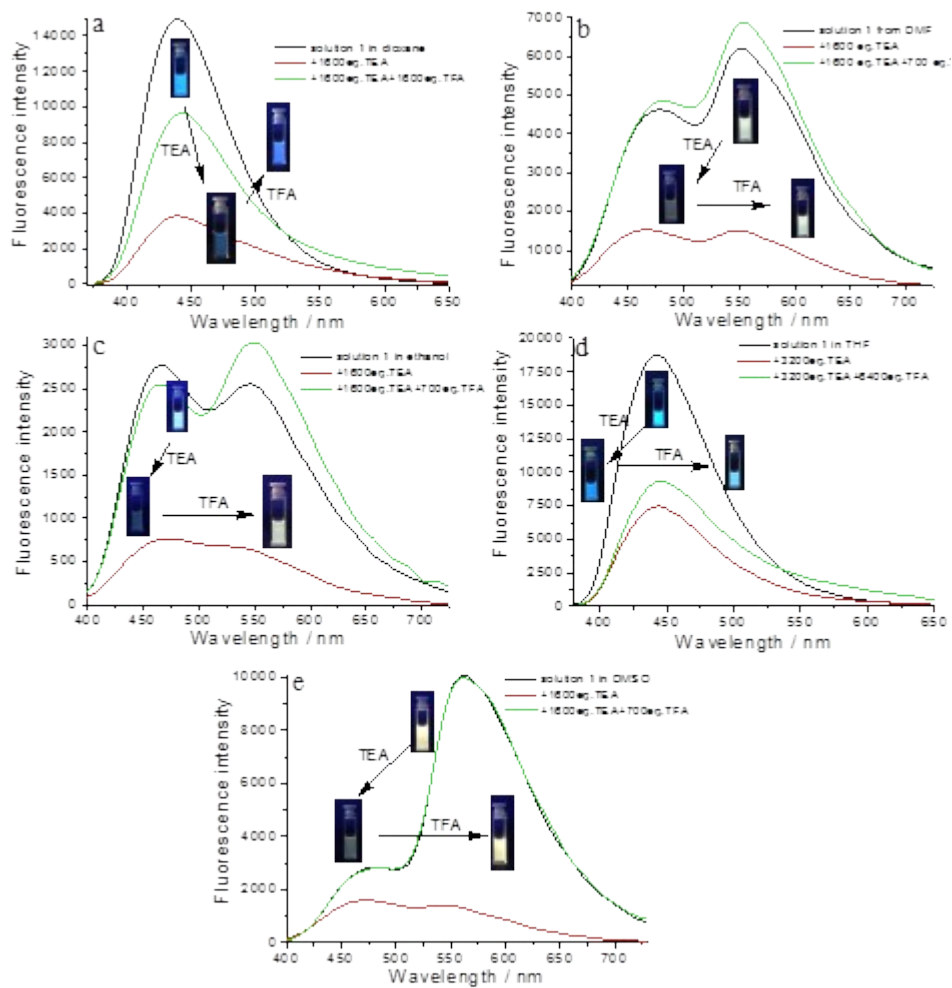


Fig. S11 Fluorescence emission change of solution 1 from different solvents under addition of TEA and further TFA at the excitation of 375 nm; a) for dioxane; b) for DMF; c) for ethanol; d) for THF and e) for DMSO. The concentration of solution 1 was 10^{-5} M.

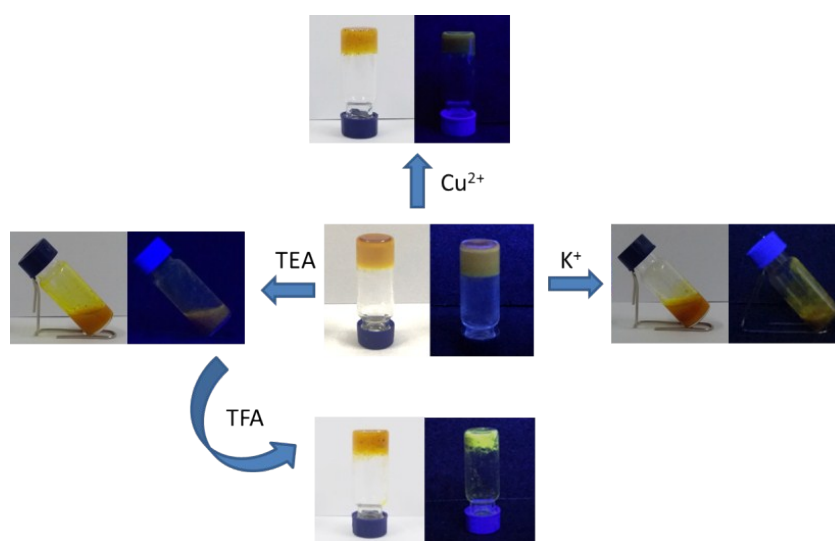


Fig. S12 Visual changes for gel 1 in acetone/H₂O (1/1, v/v) with addition of K⁺, Cu²⁺ and TEA and further TFA.

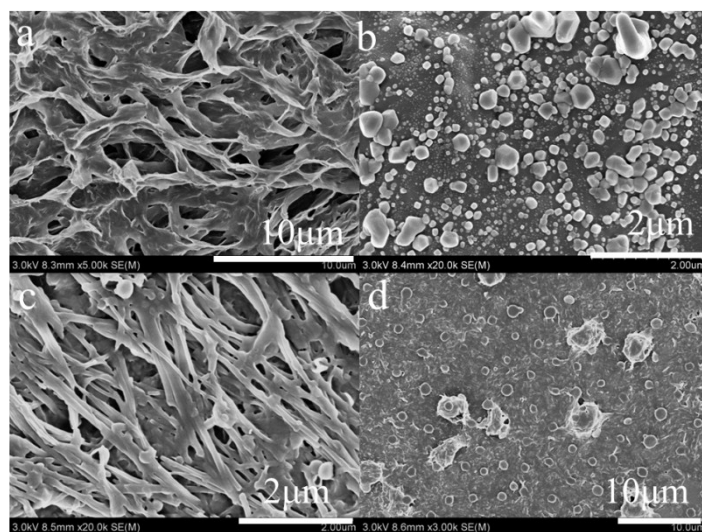


Fig. S13 SEM images of gel 1 in acetone/H₂O (1/1, v/v) with addition of K⁺, Cu²⁺ and TEA and further TFA.

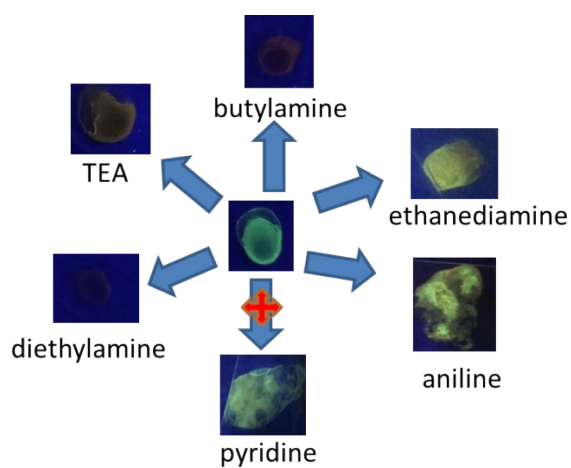


Fig. S14 Images of xerogel film 1 from acetone with different amines.

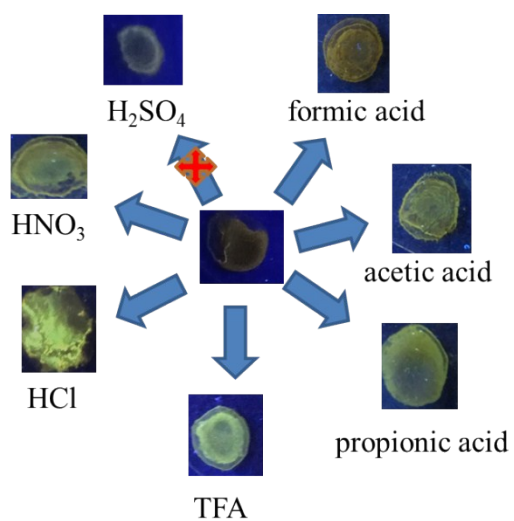


Fig.S15 Images of xerogel 1 from hexane with contacting organic amine further sensing different acids.

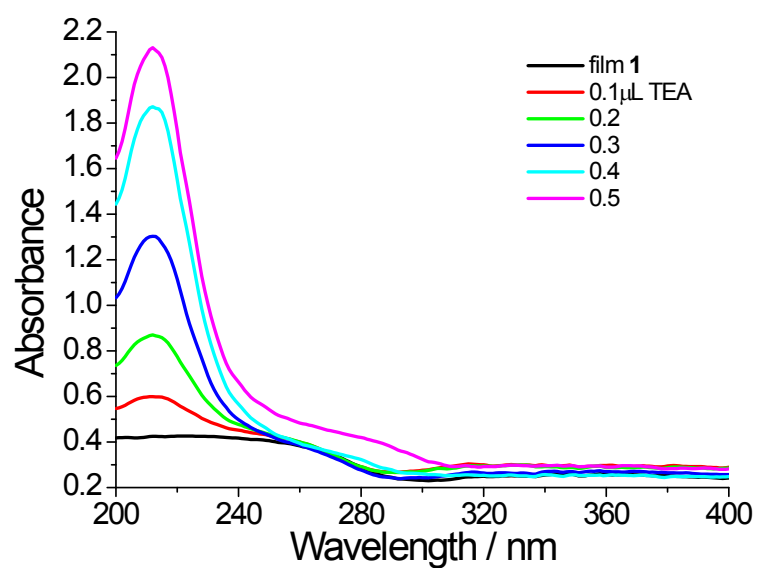


Fig. S16 The UV-vis absorption spectra of xerogel film 1 under titration of TEA gas.

Table S3 Detection limit of film 1 toward TEA in acetone by fluorescence emission changes at 522 nm

n (Xn)	1	2	3	4	5	6	7	8	9	10
intensity	324.96	323.29	323.62	324.80	324.69	324.45	324.54	323.87	323.54	323.71

$$X_{\text{average}} = 324.15 \quad \sigma_{\text{wb}} = \sqrt{\frac{\sum (X_n - X_{\text{average}})^2}{n}} = 0.32769.$$